

# DEFORMATION RESPONSE OF UNSYMMETRICALLY LAMINATED PLATES SUBJECTED TO INPLANE LOADING

Tomoya T. Ochimoto\* and Michael W. Hyer†

Engineering Science and Mechanics, Virginia Polytechnic Institute and State University, Blacksburg, VA 24061

## ABSTRACT

This paper discusses the out-of-plane deformation behavior of unsymmetric cross-ply composite plates compressed inplane by displacing one edge of the plate a known amount. The plates are assumed to be initially flat and several boundary condition cases are considered. Geometrically nonlinear behavior is assumed. The primary objectives are to study the out-of-plane behavior as a function of increasing inplane compression and to determine if bifurcation behavior and secondary buckling can occur. It is shown that, depending on the boundary conditions, both can occur, though the characteristics are different than the pre- and post-buckling behavior of a companion symmetric cross-ply plate. Furthermore, while a symmetric cross-ply plate can postbuckle with either a positive or negative out-of-plane displacement, the unsymmetric cross-ply plates studied deflect out-of-plane only in one direction throughout the range of inplane compression, the direction again depending on the boundary conditions.

## INTRODUCTION

A composite laminate is said to be symmetric if for every layer to one side of the laminate reference surface with a specific thickness, specific material properties, and specific fiber orientation, there is another layer the identical distance on the opposite side of the reference surface with identical thickness, material properties, and fiber orientation. If the laminate is not symmetric, then it is referred to as an unsymmetric laminate [1]. The terminology nonsymmetric and asymmetric are also used. There are special cases of unsymmetric laminates. One such is an antisymmetric cross-ply laminate, whereby the laminate consists of an even number of layers with the principal material directions of the layers alternating at  $0^\circ$  and  $90^\circ$  to the laminate axes. An antisymmetric angle-ply laminate has layers oriented at  $+\theta$  to the laminate coordinate axes on one side of the reference surface and layers oriented at  $-\theta$  to the laminate axes on the other side of the reference surface [2].

If a laminate is unsymmetric, then the response characteristics are somewhat unconventional due to the coupling of inplane forces with bending deformations and bending moments with inplane deformations, couplings not present in symmetric laminates. The level of asymmetry, and therefore the magnitude of the resulting elastic couplings, is determined by the lamination sequence. The higher the level of asymmetry, the higher the magnitude of the elastically-coupled responses. The level of asymmetry of a particular laminate may be evaluated by considering the laminate stiffness matrix, namely, the  $ABD$  matrix. Specifically, the  $B$  matrix, a submatrix of the  $ABD$  matrix, determines the level of coupling between the inplane and out-of-plane responses, also known as bending-stretching coupling. Laminates may be tailored to exhibit certain elastic couplings to take advantage of this unique capability. Unfortunately, traditional elevated-temperature cure techniques make it difficult to produce an unsymmetric laminate that does not change shape as it is cooled from the cure temperature [3]. As a result, flat unsymmetric laminates are difficult to manufacture. One approach is to form an unsymmetric laminate by bonding together two symmetric laminates using a room-temperature adhesive. However, due to the limitations of room-temperature adhesives and the added cost of manufacturing, this approach is of limited applicability. An alternative manufacturing method that may hold promise for the future is the electron beam curing process. Due to the low temperatures associated with this process, thermally-induced shape changes may be minimized or eliminated altogether. An even more intriguing idea would be to use nanotechnology to tailor the properties through the thickness of a flat plate to be unsymmetric.

Once flat, or curved, unsymmetric laminates can be manufactured with a degree of dimensional fidelity, attention will then focus on understanding the response of unsymmetric laminates to mechanical, and perhaps, thermal loads. The unique ability to couple inplane response with out-of-plane response will make unsymmetric laminates candidates for advanced structural tailoring concepts and possible solutions to configuration changes needed for adaptive structures not achievable by other means. Before exploring those applications, however, it will be necessary to fully characterize the response of unsymmetric laminates to simple loadings, categorize their behavior, and understand their limits. This paper is directed at these goals and will

\* Graduate Research Associate

† Professor, Associate Fellow, AIAA; Fellow, ASME; Past President, ASC

Copyright © 2002 by T.T. Ochimoto and M.W. Hyer. Published by the American Institute of Aeronautics and Astronautics, Inc., with permission.

consider the deformation response of flat unsymmetric laminates to a simple inplane compressive loading. This loading is considered because it is one of the simplest mechanical loads to model and one that can be considered in a laboratory setting. For symmetric laminates such a load would be associated with the prebuckling, buckling (bifurcation), and postbuckling behavior. For unsymmetric laminates, which, due to the elastic couplings, can begin to deform out of plane as soon as they are compressed inplane, it is not clear if the concepts of prebuckling, buckling, and postbuckling are valid. That very point is part of this investigation. Leissa [4] argued that a flat unsymmetric laminate will remain flat under a compressive inplane loading if out-of-plane rotations are restricted on all four edges, i.e., the plate is clamped. This occurs because the clamped conditions provide the moments necessary to counter the moments induced by the inplane compression which make the plate deform out of plane. If this flat state exists, then classic prebuckling, buckling, and postbuckling responses are a possibility. Leissa [5] went on to study the geometrically linear responses of four types of unsymmetric laminates subjected to uniform and linearly-varying inplane loads, including uniaxial, biaxial, and shear loads. Twelve sets of boundary conditions were considered. The result of the study was a tabulation of the center deflections of the many cases, including the case of no deflection for the conditions discussed in ref. 4. The present paper could be considered an extension to ref. 5 in that the compressive loading discussed here is one of the loadings Leissa [5] considered, and plate response into the geometrically nonlinear range is considered to further address the issues of prebuckling, buckling, and postbuckling. However, only cross-ply laminates are considered here and fewer boundary conditions are investigated, as the response of the laminates becomes complex when in the postbuckled state.

The following section describes the specific problem studied. The loading, boundary conditions, coordinate system, geometry, and nomenclature are described. As the numerical results are determined using the commercial code ABAQUS [6], finite-element considerations are also discussed. The section following that discusses numerical results.

#### PROBLEM DESCRIPTION AND ANALYSIS DETAILS

The geometry and nomenclature of the problem studied are shown in fig. 1. Rectangular plates of dimensions  $L$  by  $W$  are considered, though one square plate will be discussed. The long dimensions of the plate are referred to as the sides and the short dimensions the ends. The  $x$ -coordinate originates at one end of the plate, and the  $y$ -coordinate is centered between the two sides.

The standard principal material coordinate system for the layers is located within this coordinate system, as shown. The fiber, or 1, direction makes an angle  $\theta$  relative to the  $+x$ -axis. The displacements in the  $x$ -,  $y$ -, and  $z$ -coordinate directions are denoted by  $u$ ,  $v$ , and  $w$ , respectively. The rotations about the coordinate axes are denoted as  $\phi_x$ ,  $\phi_y$ , and  $\phi_z$ , and fig. 1 shows the sense of these rotations as defined in ABAQUS. The compressive loading is applied by displacing the right end of the plate a known amount  $U$  to shorten the plate. The associated load is denoted as  $P$ . Such a loading can be produced in the laboratory, and since it makes sense to begin any experimental investigation of the deformation response of unsymmetric laminates by considering small-scale laboratory size specimens, the plates considered are 0.508 m long by 0.406 m wide (20.0 in. by 16.0 in.). The plates are assumed to be constructed of eight-layers of graphite-epoxy and measure 1.016 mm (0.04 in.) thick. The properties of a layer are assumed to be

$$E_1 = 130.0 \text{ GPa (18.85 Msi)}$$

$$E_2 = 9.70 \text{ GPa (1.407 Msi)}$$

$$G_{12} = 5.00 \text{ GPa (0.725 Msi)}$$

$$\nu_{12} = 0.300$$

$$h = 0.1270 \text{ mm (0.005 in)}$$

Out-of-plane displacement vs. endshortening results will be presented at the three locations labeled *I*, *II*, and *III* in fig. 1. Locations *I* and *III* are quarter locations, while location *II* is at the center. Plots of the deformed geometry will be presented for specific endshortening levels. Additionally, the relationship between endshortening and the associated load  $P$  will be presented. This relation is often used for problems such as discussed here to describe the inplane stiffness of the plate as the response changes from prebuckling to postbuckling. Three combinations of boundary conditions will be prescribed along the ends and sides, and the results will be labeled SS-SS, CL-SS, and CL-CL to designate the particular boundary condition combination being considered. The terminology SS is contracted notation for simply-supported conditions and CL is a contraction for clamped conditions. The contraction to the left of the hyphen designates the prescribed boundary condition along the ends, while the contraction to the right of the hyphen designates the prescribed boundary condition along the sides. What is important to realize from the onset of the discussions is that the sides of the plates are assumed to be constrained so that  $v=0$  there. This might be considered a somewhat arbitrary and unrealistic condition, but it is also unrealistic to consider plates that might be joined with other elements to form a complete structure to have no restrictions on the  $v$ -displacements

along the sides. Rather than look at a range of elastic restraints, adding another variable to the problem, the case of full restraint is considered. This issue is important because, through Poisson effects, inplane compression in the  $x$ -direction can cause the plate to expand in the  $y$ -direction. With  $v=0$  along the sides, Poisson expansion is restricted by an inplane compression force in the  $y$ -direction. With the bending-stretching coupling present in an unsymmetric laminate, this inplane force, along with the applied inplane force, are factors.

Nine-noded, two-dimensional, geometrically-nonlinear, shear-deformable S8RS shell elements are used to model the plates. The plates are compressed statically by increasing the endshortening using very small increments of  $U$ . At each value of  $U$  the static stability of the plate is checked by examining the eigenvalues of the tangent stiffness matrix. A zero or negative eigenvalue signals a statically unstable laminate configuration. At the value of  $U$  where the static solution ceases to be stable, some iteration is then done to adjust  $U$  so that the value of  $U$  just at the onset of the instability can be closely determined. For a value of  $U$  slightly greater than this onset value, and for this value of  $U$  held fixed, a dynamic analysis, using a small amount of damping, is then initiated. For a statically unstable condition, simply initiating a dynamic analysis should be enough to allow the plate to begin to move toward a stable equilibrium configuration. However, for some unstable conditions, this requires integrating forward in time for long periods of time, as the plate may move slowly from its unstable configuration. Accordingly, as an alternative to simply initiating the dynamic analysis, the plate is given a very small pressure pulse perpendicular to the plate at time zero of the dynamic analysis. The dynamic analysis is carried out for small pressure pulses in both the  $+z$  and  $-z$  directions (see fig. 1). In general, if pressure pulses are used, the plate moves to the same configuration independent of the sign of the pressure pulse. As the plate motion is decaying around this unique configuration, the decaying being due to the light damping, a new static analysis is initiated using a decayed dynamic configuration as a starting point. The static analysis then converges within a reasonable number of iterations to what is interpreted to be the statically stable configuration for that value of endshortening. This numerical scenario corresponds to a displacement-controlled compression test in the laboratory. Ten elements in each direction, for a total of 100 elements, are used to model the plates. To test the robustness of this mesh, for several specific test cases the mesh was doubled in each direction, for a total of 400 elements. All aspects of plate response were identical for the two meshes, including the dynamic stability analysis. Of course, the dynamic stability analysis

took considerably more time with 400 elements than with 100 elements, so the 100 element mesh was used.

## NUMERICAL RESULTS

Although the goal of this paper is to investigate the response of unsymmetric composite plates, results will first be presented for an initially flat CL-SS  $[0_2/90_2]_S$  symmetric cross-ply laminate. Because it is symmetrically laminated and flat, this plate remains flat when initially loaded, and then exhibits classic bifurcation behavior. The response for this situation is well known, so relatively little new information will be presented regarding this particular plate. Rather, the results presented serve as a baseline for comparing the behavior of the initially flat  $[0_4/90_4]_T$  unsymmetric cross-ply laminate to be discussed. Also, by considering the symmetric cross-ply plate, the dynamic stability analysis implemented in ABAQUS is applied to a problem that is somewhat familiar, and the characteristics of the approach can be studied. The approach can then be applied to the unsymmetric laminate with some experience and confidence.

### $[0_2/90_2]_S$ Symmetric Cross-Ply Laminate

Figure 2 presents the normalized load vs. endshortening relation, the normalized out-of-plane displacement vs. endshortening relations, and deformed plate configurations at selected values of endshortening for the CL-SS  $[0_2/90_2]_S$  symmetric cross-ply laminate as the endshortening increases from zero to a normalized value of 10. The normalizing factor  $U_{cr}$  is the critical, or buckling, value of endshortening computed by assuming a linear, non-shear-deformable eigenvalue solution to the classic SS-SS uniaxial buckling problem [2]. The term 'classic SS-SS' implies that the boundaries are free to move inplane ( $v \neq 0$ ) and are only constrained from out-of-plane deformation ( $w=0$ ). The value of  $U_{cr}$  for the specific plate here is 0.00516 mm (0.000302 in.) and this normalizing factor was chosen simply because it is easily calculated. The CL-SS boundary conditions increases the critical endshortening with respect to the classic value, and therefore, a normalized endshortening value of 10 does not imply that the plate being discussed is compressed uniaxially to 10 times its own critical value. Strain levels in the plate were checked at  $U/U_{cr}=10$  and they were not particularly high. The normalizing factor  $P_{cr}$  used to normalize  $P$  is the load associated with  $U_{cr}$ .

The three figures for the out-of-plane displacements at points I, II, and III show that as the endshortening is increased from zero, point A, the plate remains flat. At endshortening values past point B, the plate

remains flat and is in equilibrium but it is unstable, as is well known. At a point just past point *B* in the flat configuration, the dynamic analysis is initiated. Since the plate is very close to being in a stable condition, simply integrating the equations of motion with no small pressure pulse results in a large number of time integration steps for the plate to converge to a stable equilibrium configuration. A small pressure pulse, e.g., 689 Pa (0.1 psi), applied in a ramp-up/ramp-down fashion, hastens the motion to a stable configuration characterized by a small out-of-plane displacement, as indicated by point *C* in the three figures and as shown by the leftmost deformed configuration at the bottom of fig. 2. This deformed configuration has one halfwave in the loading direction and one halfwave perpendicular to the loading direction. This, of course, is very much like the first linear buckling mode for this plate, but at point *C* the plate is in a postbuckled state. If the pressure pulse is positive, the plate moves to configuration *C*, and if the pulse is negative, the plate moves to configuration *C'*. Increasing the endshortening toward point *D*, the single half-wave configuration deepens, as shown at the bottom of the figure. Past point *D* equilibrium configurations exist but they are again unstable. Initiating a dynamic analysis just past point *D* results in the plate moving to configuration *E*. The plate could also move to configuration *E'*. If after point *B* the plate response is given by path *C'D'*, then initiating a dynamic analysis at *D'* would result in the plate also moving to configuration *E* or *E'*. As can be seen, the configurations associated with *E* and *E'* are represented by two halfwaves in the loading direction and one halfwave perpendicular to the loading direction. This change of configuration is often referred to as secondary buckling and is discussed for composite plates by Tiwari and Hyer [7]. Increasing the endshortening to point *F* deepens the configuration of point *E*. After point *B*, the slope of the normalized load vs. endshortening relation, in the upper left of fig. 2, decreases, and the relation becomes slightly nonlinear, softening as configuration *D*, or *D'*, is approached. The change to configuration *E* or *E'* is accompanied by a slight drop in load. Beyond point *E*, and *E'*, the slope of the relation decreases again.

#### $[0_4/90_4]_T$ Unsymmetric Cross-Ply Laminates

If the eight layers of the  $[0_2/90_2]_S$  symmetric cross-ply laminate are rearranged to form a  $[0_4/90_4]_T$  unsymmetric cross-ply laminate and the numerical analysis of the previous section for CL-SS boundary conditions is repeated, the normalized load vs. endshortening relation, the normalized out-of-plane displacement vs. endshortening relations, and deformed plate configura-

tions at selected values of endshortening shown in fig. 3 result. The format of fig. 3 is identical to fig. 2 to aid in a direct comparison of plate responses. A quick glance at the out-of-plane displacements at locations *I*, *II*, and *III* shows that unlike the  $[0_2/90_2]_S$  symmetric cross-ply case with multiple stable solution paths (*BCD*, *B'C'D'*, *EF* and *E'F'*), there is only one stable solution path. As the endshortening is increased from zero, the plate deforms in a stable fashion out of plane in the negative *z*-direction a very small amount. Standard experimental techniques probably could not detect any displacement, but the displacements are nonzero and the configuration at *B* is one with two halfwaves in each direction, as shown at the lower left in fig. 3. For endshortening values past point *B*, the plate is unstable and the dynamic analysis results in the plate moving to the configuration given by point *C*. Point *C* represents a large increase in the out-of-plane displacement relative to point *B*, but the configuration at Point *C*, shown at the bottom of the figure, has a configuration like point *B*. Many attempts were made to determine if the gap between points *B* and *C* is actually closed. This does not seem to be the case. With the finite-element analysis it is not possible to have the endshortening values increase continuously. However, even using fine increments in endshortening beyond point *B*, there appears to be a jump from *B* to *C*. This suggests that this particular unsymmetric laminate, with these particular boundary conditions, does not exhibit bifurcation. Increased endshortening to point *D* further deepens the halfwave configuration. For an endshortening value just past point *D*, a dynamic analysis is again initiated and stable configuration *E* results, independent of the sign of the small pressure pulse. The configuration at *E*, shown at the bottom of the figure, is not symmetric about the  $x=L/2$  line, as can be seen by comparing the out-of-plane displacement at location *I* with that at location *III*. Increased endshortening beyond configuration *E*, which exhibits negative out-of-plane displacements at all three locations, though they are relatively small at location *III*, results in a gradual transition to the configuration at point *F*. This configuration, as shown at the lower right, has a large negative out-of-plane displacement at location *I*, a smaller negative out-of-plane displacement at location *II*, and positive out-of-plane displacement at location *III*. The configuration has two halfwaves in the loading direction, but one that skewed to one end of the plate rather than being antisymmetric with respect to the  $x=L/2$  location.

If the boundary conditions on the ends of the plate are changed to be simply supported, then the responses shown in fig. 4 result. As can be seen, changing of the boundary conditions has a profound influence on the response of the plate. Specifically, as the endshortening is increased from zero the plate deforms out

of plane a significant amount. This is in contrast to the CL-SS case previously discussed in fig. 3, where the plate remained relatively flat for low end shortening levels. For the SS-SS case, as seen in the out-of-plane displacement vs. endshortening relations at locations *I*, *II*, and *III* in fig. 4, up to point *B* the plate deforms out of plane in a single halfwave configuration. At point *B*, the load vs. endshortening relation decreases slope slightly. As the endshortening is increased, the plate configuration begins to change. When the endshortening reaches the level of point *C*, the plate appears to have two halfwaves in the loading direction. A close look at the out-of-plane displacements at location *II*, however, reveals that the displacement is not zero in the center of the plate. At point *C* the plate becomes unstable, and a dynamic analysis is used to affect the transition to point *D*. At point *D* the deformed configuration looks like that at point *C*, but the out-of-plane displacement at location *II* is positive, while the magnitude of the out-of-plane displacements at locations *I* and *III* has decreased relative to point *C*. A further increase in endshortening to point *E* does not produce any configuration changes. It is clear there is nothing that resembles bifurcation behavior near point *B* in fig. 4, rather the plate configuration makes a smooth continuous shape change as the endshortening increases from *A* to *B* to *C*. Furthermore, the plate deflects out of plane in a direction opposite to the CL-SS case in fig. 3.

If instead of enforcing simply-support boundary conditions on all four sides, clamped conditions are enforced, the responses illustrated in fig. 5 occur. As the endshortening is increased from zero, the plate appears to remain flat. According to Leissa [4], this should be the case, though the finite-element results indicate there are very small out-of-plane displacements. As they are many orders of magnitude less than the out-of-plane displacements along path *AB* in fig. 3, these are felt to be a result of numerical round-off in the finite-element analysis. Increasing the endshortening past point *B* results in a statically unstable condition. The dynamic analysis leads to a statically stable equilibrium configuration whereby the plate is deformed out of plane in what appears to be a two halfwave configuration, as shown by the inset of the deformed geometry of point *C*. However, the configuration is not exactly a two halfwave one, rather there is a small out-of-plane displacement at the center of the plate, location *II*, as seen in the upper portion of fig. 5. With increasing endshortening past point *B*, the displacement at location *II* is at first negative, then positive, though it remains small. At locations *I* and *III* the displacements are much larger and have opposite signs. This psuedo-halfwave configuration remains throughout the range of endshortening studied. There is no secondary buckling behavior, as was the case for the

CL-SS and SS-SS boundary conditions of figs. 3 and 4. As was the case earlier, changing the boundary conditions relative to the CL-SS case of fig. 3, in this case making the sides clamped, has an important effect on plate response. In particular, it would appear that the plate exhibits bifurcation behavior at *B*, much like a flat symmetrically laminated plate of fig. 2. However, instead of bifurcating to positive and negative out-of-plane displacement branches, only one out-of-plane displacement branch occurs.

The psuedo-halfwave response throughout the endshortening range for the CL-CL boundary condition shown in fig. 5 is a result of the rectangular geometry of the plate. If the sidelength of the plate in fig. 5 is decreased so the plate is square, the response shown in fig. 6 results. As the endshortening is increased from zero to point *B*, the plate remains flat, to within the numerical accuracy of the analysis. At point *B* the flat configuration becomes unstable. The dynamic analysis is initiated for a flat configuration just beyond point *B* and the configuration of point *C* results. This configuration has a single halfwave in both directions. This configuration remains as the endshortening is increased to point *D*. At point *D* the single halfwave configuration becomes unstable and the dynamic analysis is again initiated. The plate assumes a configuration with two halfwaves in the loading direction and one halfwave perpendicular to that direction. Noting the nonzero displacement at location *II*, it is seen that the configuration is not truly a two halfwave one. However, as the endshortening is increased beyond point *E*, the out-of-plane displacement of the center of the plate approaches zero and the displacements at locations *I* and *III* approach being equal and opposite. For this specific configuration, bifurcation occurs at point *B*, and secondary buckling occurs at point *D*. The bifurcation results in just one out-of-plane solution branch.

## SUMMARY

This study has shown that the behavior of unsymmetrically laminated cross-ply plates subjected to inplane compression can exhibit a range of out-of-plane deformation behavior, depending on the level of compression, boundary conditions, and geometry. For this particular study the condition  $\nu=0$  was enforced along the sides, further contributing to the response. Except for the CL-CL boundary condition, the initially flat plates did not remain flat of low levels of compressive loading, though for the CL-SS case the out-of-plane displacements were very small and could be interpreted as zero in an experiment. For the CL-SS case the very small out-of-plane displacement configuration did become unstable and an alternative stable configuration was found which did have large out-of-plane displace-

ments. Secondary buckling could occur, resulting in another stable equilibrium configuration.

#### ACKNOWLEDGEMENTS

The work discussed herein was supported by grant NAG-1-2298 from the Mechanics and Durability Branch of the NASA-Langley Research Center. Dr. Damodar Ambur was the grant monitor.

#### REFERENCES

- 1 - Hyer, M.W. *Stress Analysis of Fiber-Reinforced Composite Materials*, WBC/McGraw-Hill, New York, 1998, p. 296
- 2 - Jones, R.M., *Mechanics of Composite Materials*, 2nd Ed., Taylor-Francis Publishers, Philadelphia, 1999
- 3 - Dano, M.-L. and M.W. Hyer, "Thermally-Induced Deformation Behavior of Unsymmetric Laminates," *Int. J. Solids Struct.*, 35 (17), pp. 2101-2120, 1997

4 - Leissa, A.W., "Conditions for Laminated Plates to Remain Flat under Inplane Loading," *Composite Structures*, 6, pp. 261-70, 1986

5 - Qatu, M.S. and A.W. Leissa, "Buckling or Transverse Deflections of Unsymmetrically Laminated Plates Subjected to Inplane Loads," *AIAA J.*, 31, 1, pp. 189-94, 1993

6 - ABAQUS/STANDARD. *Theory Manual*. Hibbitt, Karlsson, & Sorensen, Inc., Pawtucket, Rhode Island, 1998

7 - Tiwari, N. and M.W. Hyer, "Secondary Buckling of Laminated Composite Plates," AIAA Paper 2000-1457, presented at 41st AIAA/ASME/ASCE/AHS/ASC Structures, Structural Dynamics, and Materials Conference, Atlanta GA, April 2000, also *AIAA J.*, to be published

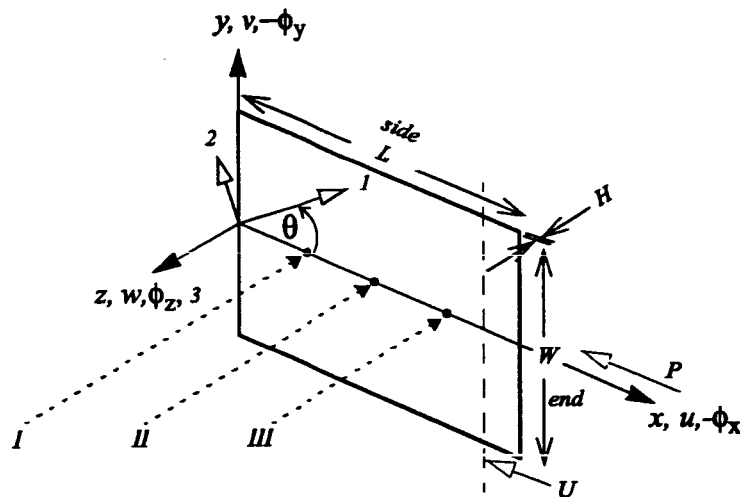


Fig. 1 - Problem description, geometry, and nomenclature

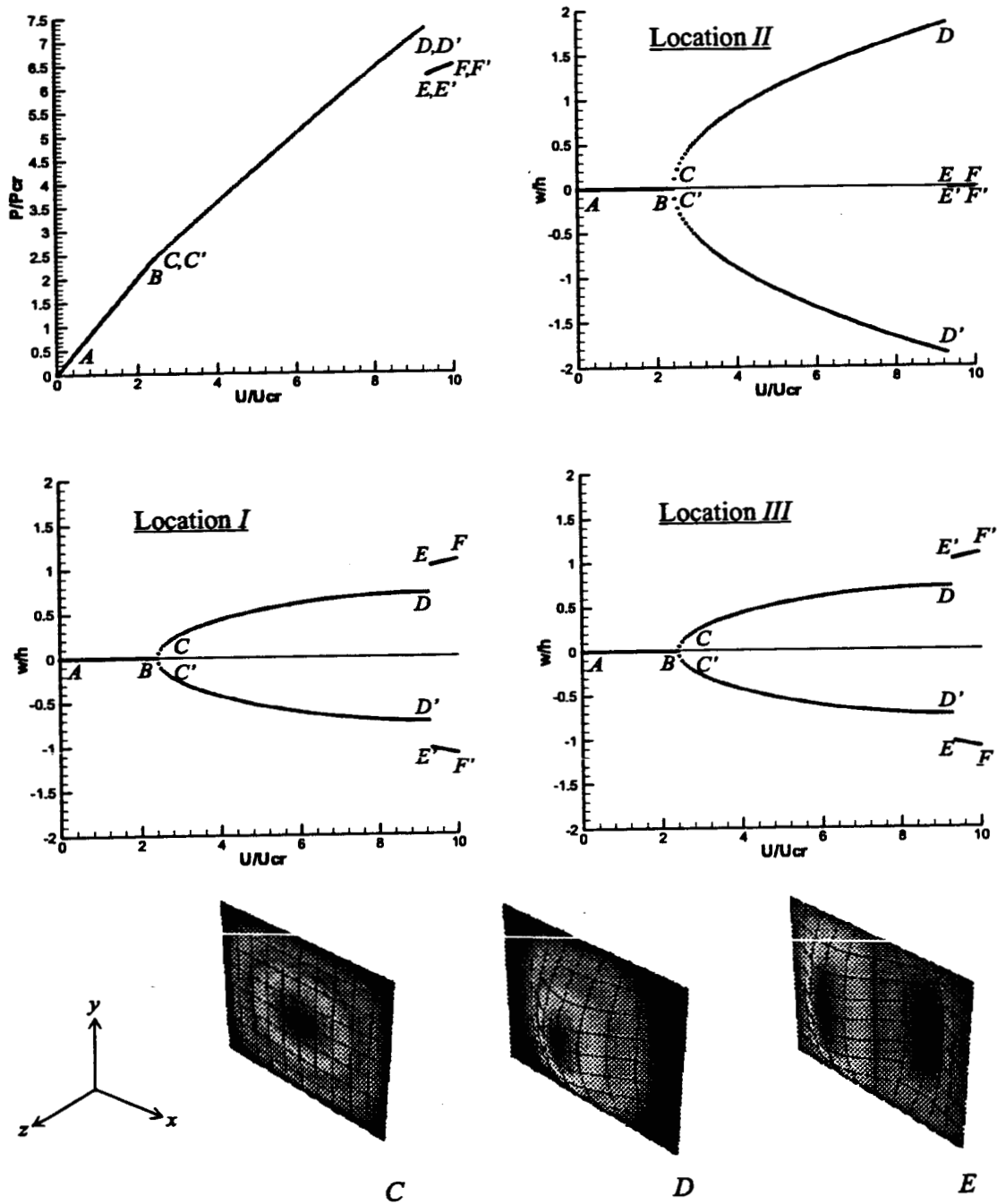


Fig. 2 - Response Characteristics of CL-SS  $[0_2/90_2]_s$  Plate

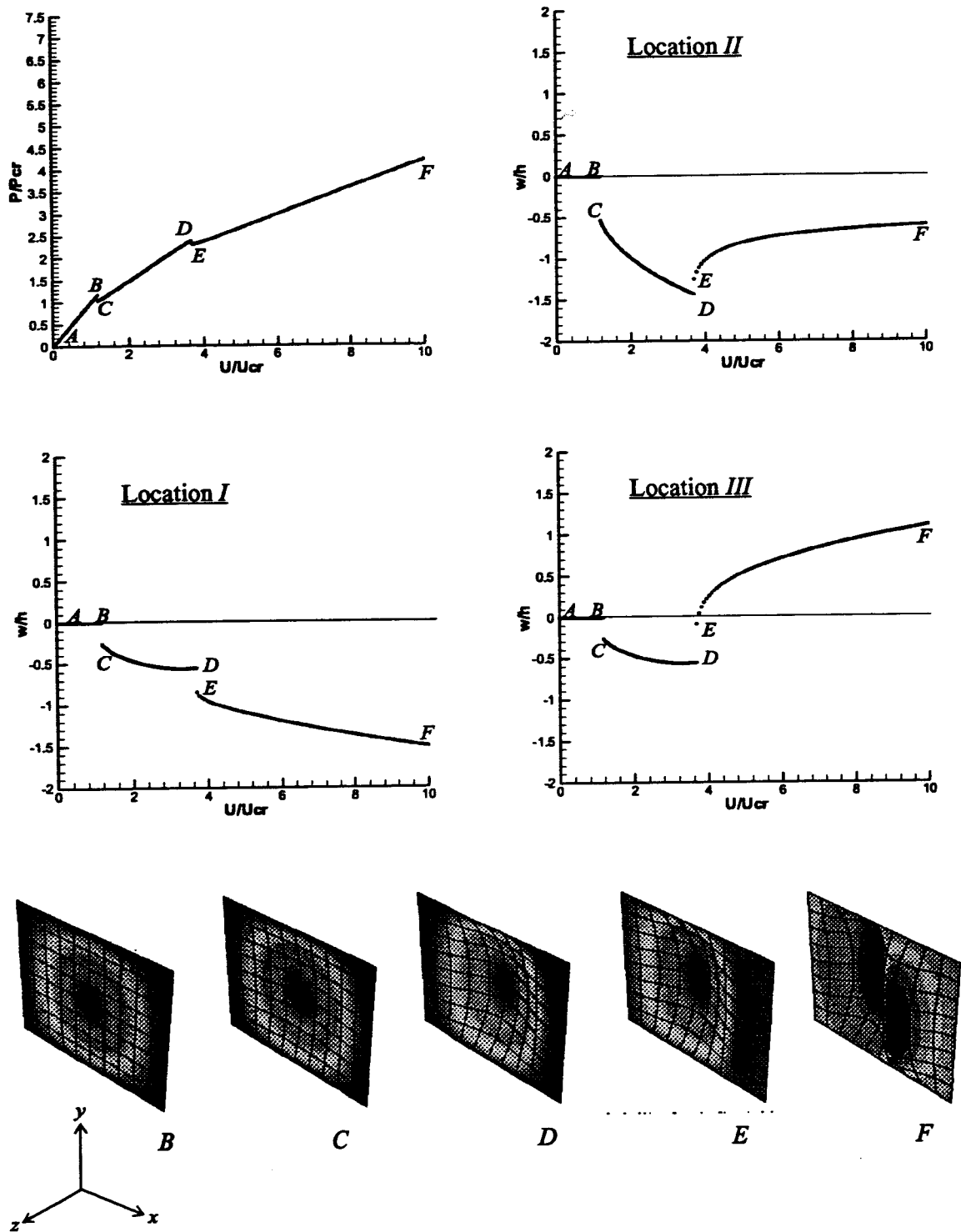


Fig. 3 - Response Characteristics of CL-SS  $[0_4/90_4]_T$  Plate



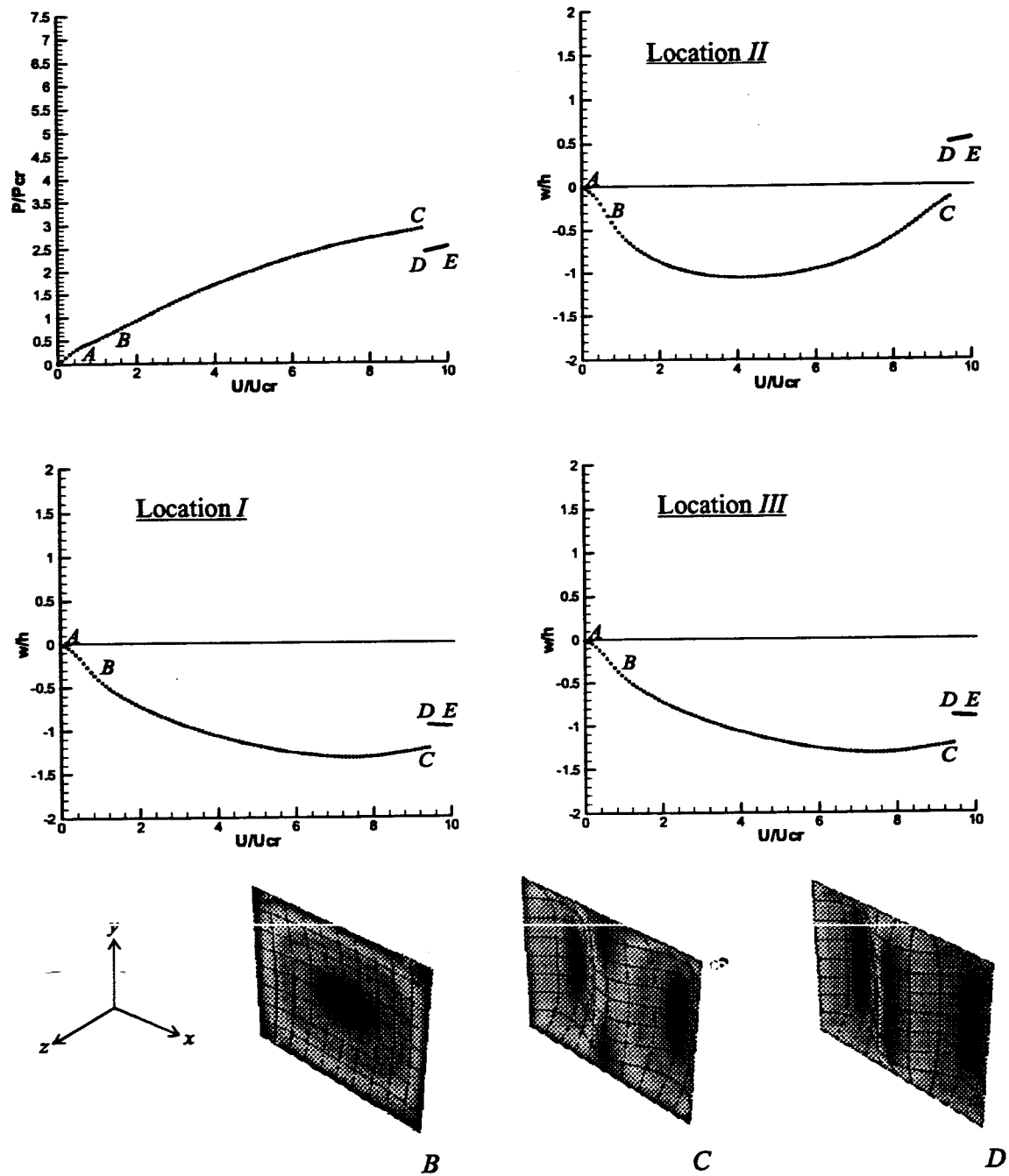


Fig. 4 - Response Characteristics of SS-SS  $[0_4/90_4]_T$  Plate

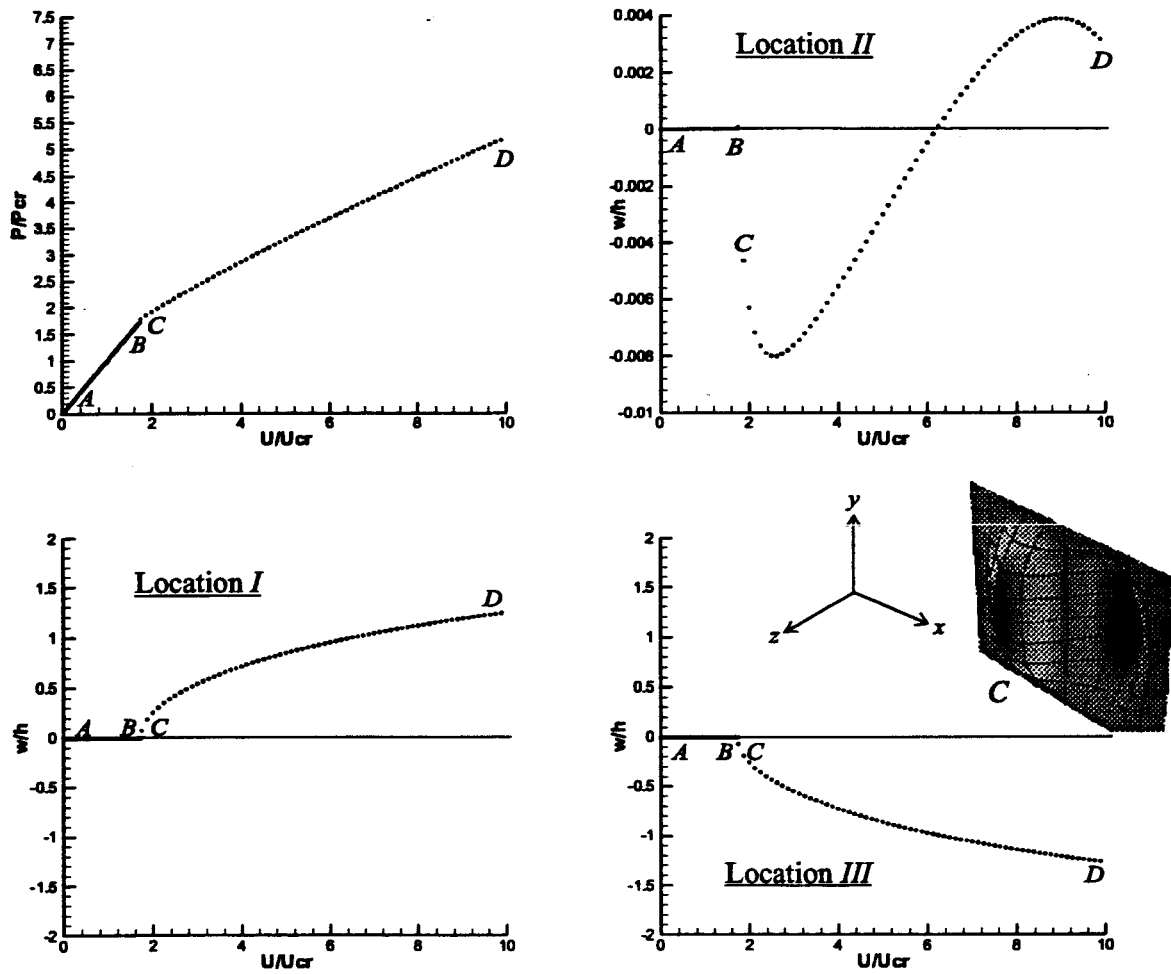


Fig. 5 - Response Characteristics of CL-CL  $[0/90_4]_T$  Plate

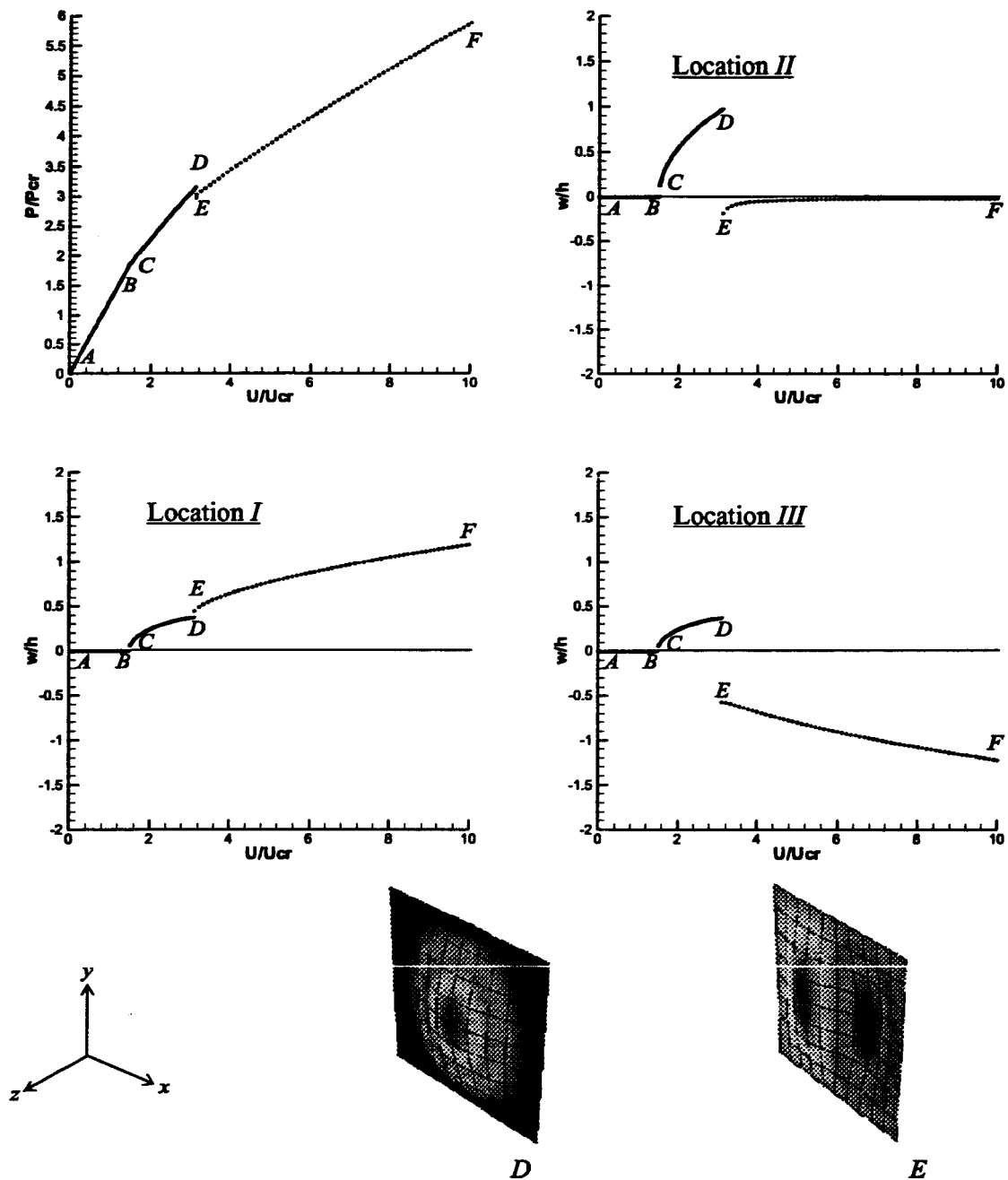


Fig. 6 - Response Characteristics of Square CL-CL  $[0_4/90_4]_T$  Plate